Journal of Nepal Mathematical Society (JNMS)
ISSN: 2616-0153 (Print), 2616-0161 (Online)
Vol. 8, Issue 2, 2025 (Dec.): 58-66
DOI: https://doi.org/10.3126/jnms.v8i2.87684

Research Article
Received Date: Sept. 15, 2025
Accepted Date: Dec. 08, 2025
Published Date: Dec. 29, 2025

Eigenvalues of the Mixture Mass Flow Model

Puskar R. Pokhrel[1,*], Tek B. Budhathoki[2,3]

[1]Tribhuvan University, Institute of Engineering, Department of Applied Sciences & Chemical Engineering, Lalitpur, Nepal
[2]Tribhuvan University, Institute of Engineering, Department of Applied Science, Thapathali Campus, Kathmandu, Nepal
[3]Tribhuvan University, Institute of Science & Technology, Central Department of Mathematics, Kirtipur, Nepal

[*]Correspondence to: Puskar R. Pokhrel, Email: puskar.pokhrel@ioe.edu.np

Abstract: *Landslides, debris flows, and tsunamis are major geophysical mass transfer dynamics that frequently occur in mountainous regions, valleys, and lower plains. This causes severe destruction of human lives, infrastructures and the environment. Understanding and predicting their behavior requires reliable modeling techniques capable of capturing the full dynamics of flow evolution, run-out distance, deposition characteristics, and impact forces from initiation to final deposition. Here, we employ the mixture mass flow model developed by Pokhrel et al. [29], to derive the characteristic equations and computing the corresponding Eigenvalues. These Eigenvalues are then used to determine the Froude number and analyze its implications in flow regimes. The resulting analysis highlights the relationship between characteristic speeds, numerical stability, and the physical behaviour of mixture mass flows. The findings enhance our theoretical understanding of mixture mass flow dynamics and contribute to practical approaches for natural hazard mitigation.*

Keywords: Mixture mass flow, Eigenvalues, Numerical stability, Froude number, Mathematical modeling.

1 Introduction

A debris flow is a gravity driven mass movement that typically consists of a mixture of loose sand, soil, rock fragments, and water, flowing down-slope predominantly gravitational forces[13, 14, 27, 34, 36]. Debris flows which generally occur in mountainous regions worldwide, are extremely destructive and hazardous geophysical mass movement events. They may also be triggered by sudden surges of water generated by dam failures, rockfalls, or landslides into lakes, oceans, or rivers, causing rapid overflow and subsequent mobilization of loose material[7, 23, 24, 25, 35]. As a flood wave travels down a dry or weakly saturated channel, it may evolve into a debris flow by eroding the bed and entertaining additional solid material along on its path [12, 21]. During the motion, the mixture material undergoes with rapid deformations, strong nonlinear interactions, and continuously evolving flow boundaries. In steep terrain, some debris flows can reach extreme velocities, often exceeding 160 km/h, making them particularly dangerous [18]. From a modeling perspective, debris flows are described as gravity-driven movements of material consisting of multi-phase flows[13, 14, 27, 30, 33, 34, 36]. For modeling avalanches and debris flows, Pitman and Le [27] introduced a two-fluid model, whereas Fernandez-Nieto et al. [10] formulated a two-layered model. Pudasaini [33] developed a generalized two-phase model that captures all major physics of mixture flows, including buoyancy and strong phase interactions. This model incorporates three key mechanisms: enhanced non-Newtonian viscous stress due to solid volume fraction gradients, virtual mass forces and generalized drag forces. Kattel and Tuladhar [17] examined the flow dynamics, wall-flow interactions and phase-wise run out morphology by using the two-phase model developed by Pudasaini [33]. Pokhrel et al. [29] developed a mixture mass flow model that captures all essential physics, incorporates with mixture viscosity effects in terms of drift dynamics, and enables fast and efficient numerical solution.

Liu and Ortiz [20] investigated the Eigenvalue problem for partial differential equations with constant coefficients, while Leipnik [19] determined the Eigenvalues of partial differential equations by formulating the corresponding characteristic equations and analyzing their sensitivity and perturbation behavior. Boumenir [3] proved a conjecture concerning certain Eigenvalues of the periodic Sturm-Liouville problem (a second order differential equation). Wang and Shen [38] established the existence of the Eigenvalues for second order differential equations with impulses. Pudasaini [33] analyzed the dynamics of two-phase mass flows by performing a detailed Eigenvalue analysis of his generalized model. Based on the generalized model, [33],

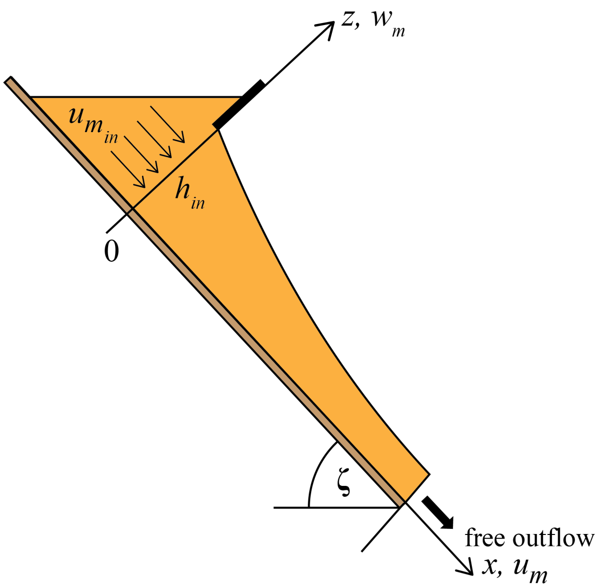

Figure 1: Initial setup showing the mixture's inlet velocity $u_{m_{in}}$, flow height h_{in}, and chute inclination angle ζ [29].

Pokhrel and Tuladhar [28] derived the phase-wise Eigenvalues of the governing partial differential equations, and demonstrated that these Eigenvalues significantly improve the understanding of flow dynamics, including the estimation of wave speeds and Froude numbers. In this paper, based on the mixture mass flow model developed by Pokhrel et al. 2018 [29], we aim to establish a comprehensive understanding of the Eigenvalues, Froude number, and Courant Friedrichs Lewy (CFL) condition through numerical simulations of scenarios with varying sizes and volumes of initial debris mass.

2 Physical Mathematical Model and Numerical Methods

The mixture mass flow model developed by Pokhrel et al. [29] is expressed as

$$\frac{\partial u_m}{\partial x} + \frac{\partial w_m}{\partial z} = 0, \tag{1}$$

$$\frac{\partial u_m}{\partial t} + \frac{\partial}{\partial x}(\Lambda_{uu} u_m^2) + \frac{\partial}{\partial z}(\Lambda_{uw} u_m w_m) = g\,\cos\zeta - \frac{\partial p_m}{\partial x} + 2\frac{\partial}{\partial x} + \left[\Lambda_{\eta_u}\frac{\partial(\Lambda_u u_m)}{\partial x}\right]$$
$$+ \frac{\partial}{\partial z}\left[\Lambda_{\eta_u}\frac{\partial(\Lambda_u u_m)}{\partial z} + \Lambda_{\eta_w}\frac{\partial(\Lambda_w w_m)}{\partial x}\right], \tag{2}$$

$$\frac{\partial w_m}{\partial t} + \frac{\partial}{\partial x}(\Lambda_{wu} u_m w_m) + \frac{\partial}{\partial z}(\Lambda_{ww}\, w_m^2) = g\sin\zeta - \frac{\partial p_m}{\partial z} + \frac{\partial}{\partial x}\left[\Lambda_{\eta_u}\frac{\partial(\Lambda_u u_m)}{\partial z} + \Lambda_{\eta_w}\frac{\partial(\Lambda_w w_m)}{\partial x}\right]$$
$$+ 2\frac{\partial}{\partial z}\left[\Lambda_{\eta_w}\frac{\partial(\Lambda_w w_m)}{\partial z}\right], \tag{3}$$

where u_m and w_m are the down-slope and perpendicular mixture velocities (Fig. 1), t is time, and p_m is the mixture pressure. The mixture velocities and pressure are defined as [29]:

$$u_m = (\alpha_s + \lambda_u \alpha_f)u_s, \;\; w_m = (\alpha_s + \lambda_w \alpha_f)w_s, \;\; p_m = (\alpha_s + \lambda_p \alpha_f)p_s,$$

with λ_u, λ_w as velocity drift factors, and λ_p as pressure drift factor. The coefficients Λ_u and Λ_w are determined by

$$\Lambda_u = \frac{1}{\alpha_s + \lambda_u \alpha_f}, \;\; \Lambda_w = \frac{1}{\alpha_s + \lambda_w \alpha_f}.$$

α_s, $\alpha_f(= 1 - \alpha_s)$, are the solid and fluid volume fractions, with p_s and p_f respective phase pressures. $\mathbf{f} = (f_x,\, f_z)$ represents the gravitational acceleration, and the mixture viscosities are $\Lambda_{\eta_u} = \nu_s^e \alpha_s + \lambda_u \nu_f \alpha_f$, $\Lambda_{\eta_w} = \nu_s^e \alpha_s + \lambda_w \nu_f \alpha_f$, where ν_s^e and ν_f are the solid and fluid kinematic viscosities. The inertial coefficients are

$$\Lambda_{uu} = \frac{\alpha_s + \lambda_u^2 \alpha_f}{(\alpha_s + \lambda_u \alpha_f)^2}, \;\; \Lambda_{ww} = \frac{\alpha_s + \lambda_w^2 \alpha_f}{(\alpha_s + \lambda_w \alpha_f)^2}, \;\; \Lambda_{uw} = \frac{\alpha_s + \lambda_u \lambda_w \alpha_f}{\alpha_s + \lambda_u \alpha_f}, \;\; \Lambda_{wu} = \frac{\alpha_s + \lambda_u \lambda_w \alpha_f}{\alpha_s + \lambda_w \alpha_f}.$$

Our newly derived Eigenvalues, together with resulting CFL condition, and the Froude number obtained from them, play a central role in the numerical computation of the mixture mass flow model. The CFL condition is employed in the numerical simulations to ensure stability. The simulations of the model are performed using the extended *Nast2D* method [8, 9, 11]. This numerical method is an advanced computational code based on finite volume for simulating the complex mixtures of incompressible non-Newtonian fluids and granular particles. The computational domain is discretized using a staggered grid to prevent pressure oscillations. Numerical instabilities are minimized by employing a combination of central difference and donor-cell discretization schemes. The flow domain along x- and z- axes is divided into a large number of equally sized cells for accurate computation. In this domain, p_m is at the cell centers, u_m along x- axis at vertical edge midpoints, and w_m along z- axis at horizontal edge midpoints.

3 Results and Discussion

3.1 Characteristic Equation

For an $n \times n$ matrix A, if $AX = \lambda X$ for some vector X and scalar λ, then λ is an Eigenvalue of A, and the corresponding (right) X is its Eigenvector. The equation $det(A - \lambda I) = 0$ is said to be characteristic equation, which provides the Eigenvalues of the matrix A, where I is the identity matrix of order n. For our mixture mass flow model as a set of non-linear partial differential equations (1) - (3), the corresponding Eigenvalues of the system are obtained as the roots of the characteristic equation. The matrix A arises from the spatial derivative of the flux vector $\mathbf{F}$ with respect to the conservative variables. The resulting Eigenvalues are significant because they determine the characteristic wave speeds needed to satisfy the CFL (Courant-Friedichs-Lewy) stability criterion[6]. The CFL condition ensures numerical stability of the simulations. From the Eigenvalues, we also compute Froude number that characterizes the critical flow states. The Froude number is essential for designing civil and protective structures exposed to geophysical mass flows. In particular, for hazards such as landslides, avalanches and debris flows, these numbers play a key role in determining the design and effectiveness of defense structures [8, 9, 28]. Let $\mathbf{u}_m = (u_m,\, w_m)^T$ denote the velocity field, with u_m and w_m as the x- and z- directions components. The flux tensor is given by

$$\mathbf{F}(\mathbf{u}_m) = \begin{bmatrix} \Lambda_{uu} u_m^2 & \Lambda_{uw} u_m w_m \\ \Lambda_{wu} w_m u_m & \Lambda_{ww} w_m^2 \end{bmatrix} \tag{4}$$

The gravitational force vector $\mathbf{g}$ is given by

$$\begin{bmatrix} g^x \cos\zeta \\ g^z \sin\zeta \end{bmatrix}.$$

The stress tensor is

$$\mathbf{T} = \begin{bmatrix} 2\Lambda_{\eta_u} \frac{\partial}{\partial x}\left(\Lambda_u u_m\right) & \Lambda_{\eta_u} \frac{\partial}{\partial z}\left(\Lambda_u u_m\right) + \Lambda_{\eta_w} \frac{\partial}{\partial x}\left(\Lambda_w w_m\right) \\ \Lambda_{\eta_u} \frac{\partial}{\partial z}\left(\Lambda_u u_m\right) + \Lambda_{\eta_w} \frac{\partial}{\partial x}\left(\Lambda_w w_m\right) & 2\Lambda_{\eta_w} \frac{\partial}{\partial z}\left(\Lambda_w w_m\right) \end{bmatrix}$$

The matrix A is obtained by the partial derivative of $\mathbf{F}$:

$$A = \frac{\partial \mathbf{F}}{\partial \mathbf{u}_m} = \begin{bmatrix} 2\Lambda_{uu}u_m & \Lambda_{uw}u_m \\ \Lambda_{wu}u_m & 0 \end{bmatrix}.$$

Let λ be the Eigenvalue, then the characteristic equation is given by $\det(A - \lambda I) = 0$ gives

$$\begin{vmatrix} 2\Lambda_{uu}u_m - \lambda & \Lambda_{uw}u_m \\ \Lambda_{wu}u_m & 0 - \lambda \end{vmatrix} = 0,$$

$$\text{or} \qquad \lambda^2 - 2\Lambda_{uu}u_m\lambda - \Lambda_{wu}\Lambda_{wu}w_m^2 = 0.$$

4 Eigenvalues and Applications

4.1 Applications of Eigenvalues

For the non-linear partial differential equations (1) - (3), Eigenvalues provide important insights into the system, and are obtained from the characteristic equations, giving

$$\lambda = \frac{2\Lambda_{uu}u_m \pm \sqrt{4\Lambda_{uu}^2 + 4\Lambda_{uw}\Lambda_{wu}w_m^2}}{2} = \Lambda_{uu}u_m \pm \sqrt{\Lambda_{uu}^2 + \Lambda_{uw}\Lambda_{wu}w_m^2}.$$

Thus, the coupled Eigenvalues are

$$\lambda_{1,2} = \Lambda_{uu}u_m \pm \sqrt{\Lambda_{uu}^2 + \Lambda_{uw}\Lambda_{wu}w_m^2}.$$

In this discussion, two practical aspects are highlighted where Eigenvalues play a fundamental role in describing the physics of mixture flows and their analysis. These aspects are associated with numerical stability and critical flows. Both of these aspects are crucial in designing of defense structures.

4.2 Numerical Stability Analysis

The CFL (Courant-Friedrichs-Lewy) condition is essential for preventing un-physical oscillations and maintaining the stability of numerical schemes, thereby ensuring accurate and reliable simulations of mixture flows. The CFL condition is determined using the Eigenvalues derived from the equations (1) - (3). These Eigenvalues help to establish the relationship between the maximum wave speed and the numerical stability condition, as described in [28, 33]:

$$\frac{\triangle t}{\triangle x}\,|C^{max}| < \frac{1}{2}, \qquad \text{where} \;\; C^{max} = max\{\lambda_1, \lambda_2\}.$$

In these expressions, $\triangle t$ and $\triangle x$ denote the temporal and spatial spacing of the numerical grid, and λ_1 and λ_2 be the Eigenvalues of the mixture flow model equations, defined as:

$$\lambda_1 = \Lambda_{uu}u_m - \sqrt{\Lambda_{uu}^2 + \Lambda_{uw}\Lambda_{wu}w_m^2},$$
$$\lambda_2 = \Lambda_{uu}u_m + \sqrt{\Lambda_{uu}^2 + \Lambda_{uw}\Lambda_{wu}w_m^2}.$$

These Eigenvalues are novel and play a crucial role in determining the CFL condition to simulate the mixture flows down an inclined channel.

4.3 Flow Characteristics

Eigenvalues influence the classification of flow regimes, particularly through the Froude number, which is crucial for understanding flow transitions and designing effective defense structures against natural hazards. By analyzing Eigenvalues, we gain deeper insights into the stability and behavior of mixture flows, contributing to both theoretical advancements and practical engineering applications. The Froude number (Fr) is a key dimensionless parameter that characterizes the dynamics of free surface gravity flows [8]. It

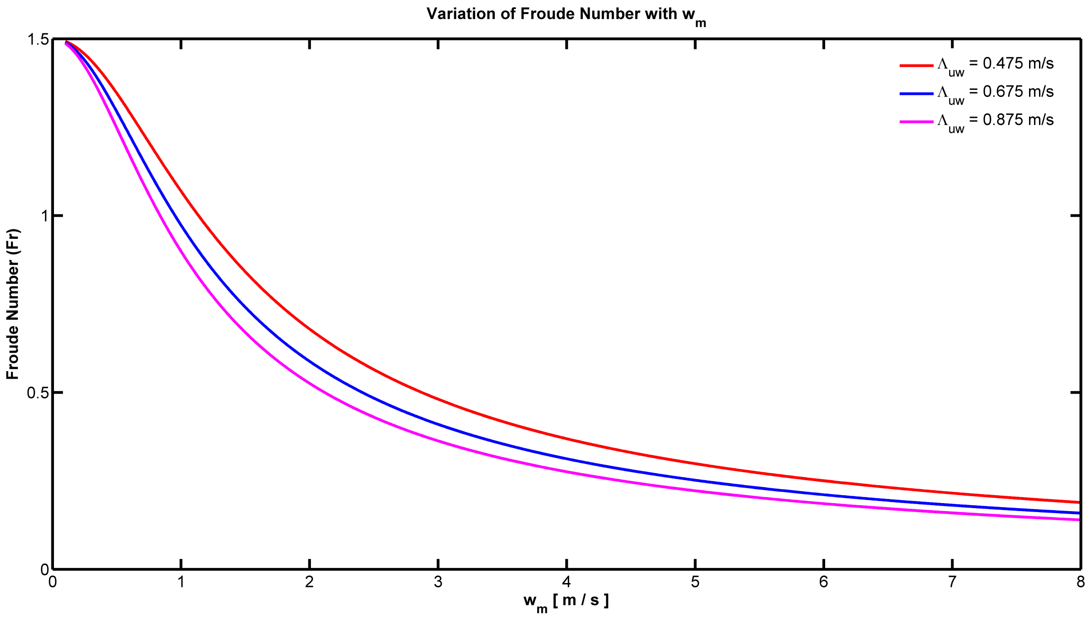

Figure 2: Flow regimes classified based on the determination of the Froude number using Eigenvalues.

distinguishes sub-critical ($Fr < 1$), critical ($Fr = 1$), and supercritical ($Fr < 1$) flow regimes [28]. In classical free-surface or granular flows on inclined slopes, Fr is defined as the ratio of inertial to gravity forces or equivalently, of kinetic to potential energy. It is widely used to establish dynamic similarity between laboratory-scale and full-scale flows, for example in the design of avalanche protection dams and weirs[8]. The advancement of this formulation is achieved by constructing coupled mixture Froude numbers for the solid and fluid components. The classical Froude numbers compare inertial forces to gravitational forces and is usually in the form:

$$Fr = \frac{velocity}{\sqrt{g\,L}},$$

where g is the gravitational acceleration and L is a typical length scale. In the context of mixture mass flows, gravitational effects are implicitly incorporated through the phase-interaction parameters Λ_{uu}, Λ_{uw}, and Λ_{wu}, the interaction coefficients λ_u and λ_w, and the volume fractions of the solid and fluid phases, α_s and α_f. As a result, the generalized Froude number for the mixture mass flow, associated with Eigenvalues of the system is

$$Fr = \frac{\Lambda_{uu}\, u_m}{\sqrt{\Lambda_{uu}^2 + \Lambda_{uw}\Lambda_{wu} w_m^2}}.$$

This Froude number represents a novel result for the mixture model equations, providing a key parameter for characterizing the dynamics and behavior of mixture flows.

4.4 Froude Number and Flow Regimes

The derived Eigenvalues λ_1 and λ_2 provide essential information on the characteristic speeds of wave propagation in the mixture flow system. These Eigenvalues not only define the propagation direction and magnitude of information through the flow field but also play a pivotal role in setting up the CFL condition for stable numerical simulations of the mixture flow model, particularly over inclined channels.

The generalized Froude number introduces a novel approach for classifying flow regimes in mixture mass flow systems. Analogous to its classical counterpart, it measures the relative dominance of inertial forces over gravitational influences. However, it does so in a way that accounts for the internal coupling between solid and fluid phases-embedded through the parameters Λ_{uu}, Λ_{uw} and Λ_{wu}. Subcritical flow corresponds to $Fr < 1$ gravitational effects dominate. Supercritical flow corresponds to $Fr > 1$ inertial effects dominate, and the critical flow occurs at $Fr = 1$, a transition regime where wave speeds and flow speeds coincide.

Figure 2 illustrates the variation of the Froude number, Fr with the normal velocity w_m when the velocity

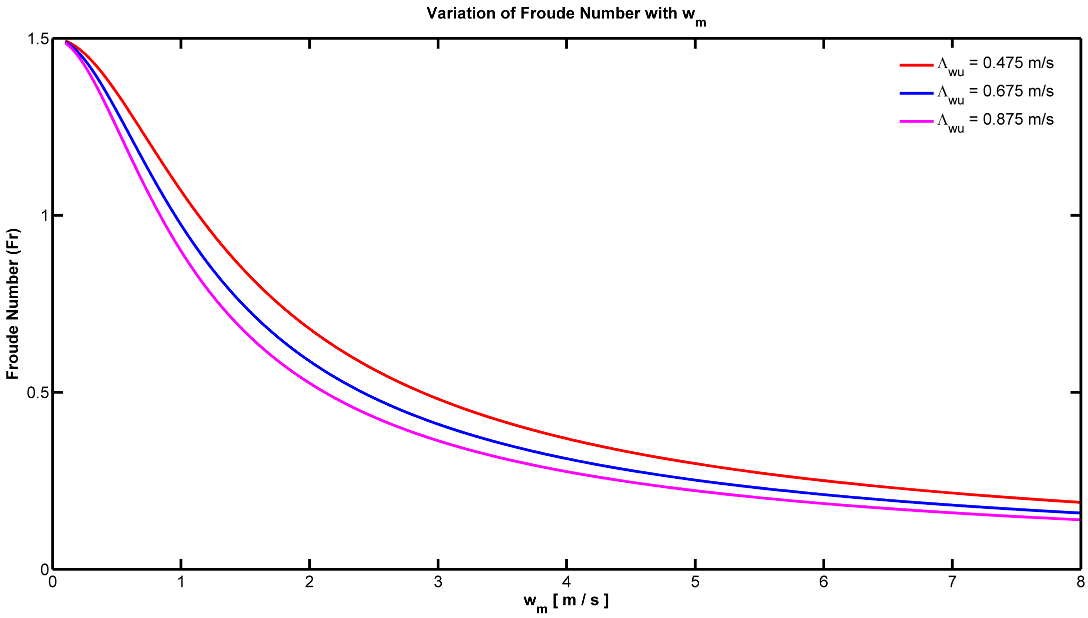

Figure 3: Flow regimes classified based on the determination of the Froude number using Eigenvalues.

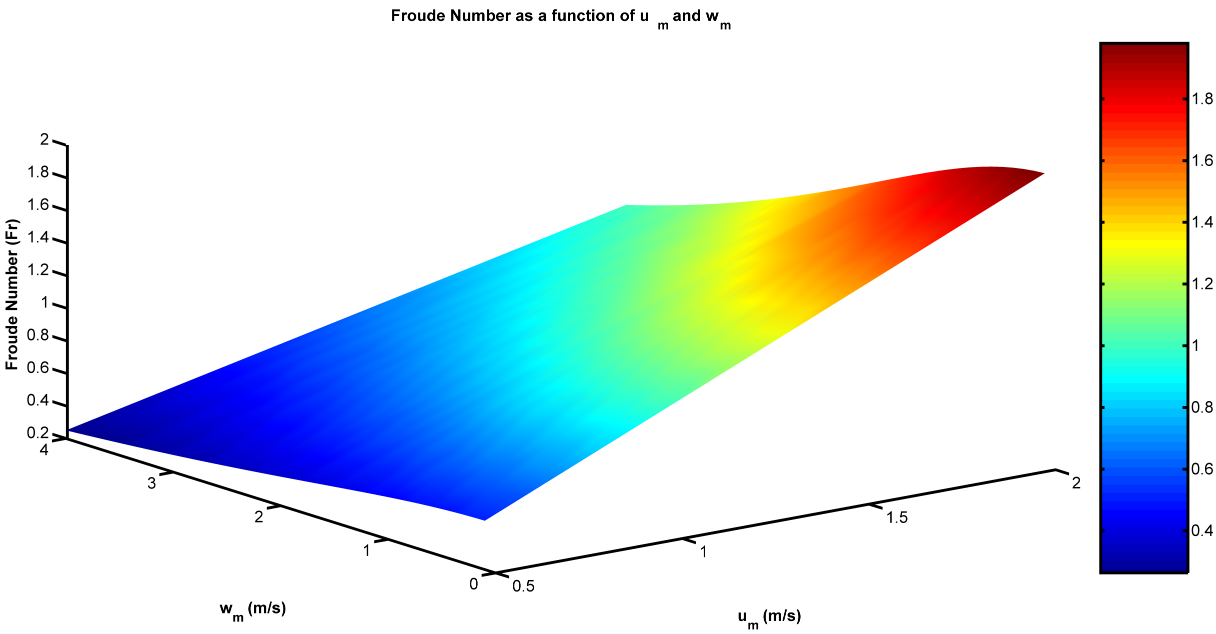

Figure 4: Froude number derived from the Eigenvalues as a function of mixture velocities u_m and w_m.

along the mixture mass flow direction is fixed at $u_m = 1.5$ m /s, and the parameters $\Lambda_{uu} = 0.350$ m^2/s^2 and $\Lambda_{uw} = 0.250$ m/s are held constant. The plot compares the effect of varying Λ_{wu} values (0.475 m/s, 0.675 m/s, and 0.875 m/s) on the critical state of the flow. Specifically, the flow reaches the critical condition ($F_r = 1$) at approximately: $w_m = 1.2$ m/s for $\Lambda_{wu} = 0.875$ m / s, $w_m = 1.4$ m/s for $\Lambda_{wu} = 0.675$ m / s, and $w_m = 1.6$ m/s for $\Lambda_{wu} = 0.475$ m / s. As the normal velocity w_m increases- while u_m, Λ_{uu}, and Λ_{uw} remain fixed, the Froude number F_r decreases below 1, indicating a transition from supercritical to subcritical flow. This behavior highlights that although the streamwise velocity u_m and the parameters Λ_{uu} and Λ_{uw} are constant, an increase in the normal velocity w_m leads to subcritical flow condition($F_r < 1$).

Figure 3 shows how the Froude number (F_r) varies with the normal velocity w_m under different values of the parameter Λ_{wu} with fixed parameters $\Lambda_{uw} = 0.250$ m/s and $\Lambda_{uu} = 0.350$ m^2/s^2, and $u_m = 1.5$ m /s. The plot contains three curves (red, blue, magenta), each representing one of the values Λ_{wu} (0.475 m/s, 0.675 m/s, and 0.875 m/s). As w_m decreases for all cases, meaning the flow transitions toward a subcritical regime ($F_r < 1$). Higher Λ_{wu} values result in a faster drop in $F_r < 1$, reaching the critical state ($F_r = 1$) at lower w_m values. Specifically, for $\Lambda_{wu} = 0.875$ m / s, critical state is reached at lower w_m than for 0.675 m / s, or 0.475 m / s. Figure 3 demonstrates how the Froude number behavior depends on both normal velocity and coupling parameters (Λ_{wu}, Λ_{uw}, and Λ_{uu}), highlighting the transition between supercritical and subcritical flow regimes in the mixture mass flow system.

Figure 4 represents a smooth surface with interpolated shading, giving a continuous three dimensional view. A colorbar is added to show the scale of Fr values. Let u_m, w_m represent horizontal and vertical velocities along x-, and z- axes respectively, and the Froude number F_r represents along the z- axis. As u_m increases, the Froude number F_r increases linearly (because it appears directly in the numerator). As w_m increases, the Froude number F_r decreases (because it increases the denominator under the square root, reducing the overall value). The combined surface shape highlights how the flow transitions from supercritical ($F_r > 1$) to subcritical ($F_r < 1$) regimes depending on the balance between u_m and w_m.

Therefore, Figure 4 provides a three dimensional visualization of how horizontal and vertical velocity components jointly control the Froude number, which is important for understanding flow regimes, stability, and the transition between critical states in mixture mass flows. This formulation enables the study of wave interactions, shock formation, and interface dynamics within multi-phase mixtures, offering a more complete understanding of debris flows, landslides, or sediment transport phenomena.

5 Conclusions

In this paper, a novel formulation of the generalized Froude number has been developed for mixture mass flow systems, incorporating the complex interactions between solid and fluid phases through the coupling parameters Λ_{uu}, Λ_{uw}, and Λ_{wu}, as well as the interaction coefficients λ_u, λ_w, and volume fractions α_s, α_f. The resulting Eigenvalues of the governing equations capture the characteristic wave speeds in the mixture and form the basis for determining stable numerical simulation condition through the CFL criterion. The generalized Froude number serves as a key diagnostic tool for identifying flow regimes - subcritical, supercritical, and critical, in two-phase flow environments. This framework not only generalizes the classical Froude number but also enhances the theoretical foundation for simulating and understanding real-world geophysical mixture mass flows, and other complex granular-fluid interactions on inclined terrains.

References

[1] Audusse, E., 2005, A multilayer Saint-Venant model: Derivation and numerical validation, *Discrete Cont. Dyn. Syst., Ser.*, B 5(2), 189-214.

[2] Bouchut, F., and Morales, T., 2008, An entropy satisfying scheme for two layer shallow water equations with uncoupled treatment, *ESAIM: Math. Modell. Numer. Anal.*, 42(4), 683-698.

[3] Boumenir, A., 1999, A rigorous verification of a numerically computed eigenvalue, *Computers and Mathematics with Applications*, 38(7-8), 39–41.

[4] Castro, M., Frings, J. T., Noelle, S., Pares, C., and Puppo, G., 2010, On the hyperbolicity of two- and three-layer shallow water equations, *Inst. für Geom. und Prakt. Math. Aachen Univ.*, Report 314, 1-8.

[5] Castro-Diaz, M. J., Fernandez-Nieto, E. D., Gonzalez-Vida, J. M., and Pares-Madronal, C., 2011, Numerical treatment of the loss of hyperbolicity of the two-layer shallow-water system, *J. Sci. Comput.*, 48(13), 16-40.

[6] Courant, R., Friedrichs, K. O., and Lewy, H., 1967, On the partial differential equations of mathematical physics, *IBM J. Math. Ann.*, 11, 215-234.

[7] Crosta, G. B., Chen, H., and Lee, C. F., 2004, Replay of the 1987 Val Pola landslide, *Italian Alps. Geomorphology*, 60(12), 127-146.

[8] Domnik, B., and Pudasaini, S. P., 2012, Full two-dimensional rapid chute flows of simple viscoplastic granular materials with a pressure-dependent dynamic slip-velocity and their numerical simulations, *J. Non-Newtonian Fluid Mech.*, 173-174, 72-86.

[9] Domnik, B., Pudasaini, S. P., Katzenbach, R., and Miller, S. A., 2013, Coupling of full two-dimensional and depth-averaged models for granular flows, *J. Non-Newtonian Fluid Mechanics*, 201, 56-68.

[10] Fernandez-Nieto, E. D., Bouchut, F., Bresch, D., Castro Daz, M. J., and Mangeney, A., 2008, A new Savage-Hutter type model for submarine avalanches and generated tsunami, *J. Comput. Phys.*, 227(16), 7720-7754.

[11] Griebel, G., Dornseifer, T., and Neunhoeffer, T., 1997, *Numerical Simulation in Fluid Dynamics: A Practical Introduction*, Society for Industrial and Applied Mathematics, Philadelphia.

[12] Iverson, R. M., 2012, Elementary theory of bed-sediment entrainment by debris flows and avalanches, *J. Geophys. Res.*, 117 (F03006), 197-200.

[13] Iverson, R. M., and Denlinger, R. P., 2001, Flow of variably fluidized granular masses across three-dimensional terrain: 1. Coulomb mixture theory, *J. Geophys. Res.*, 106(B1), 537-552.

[14] Johnson, A. M., 1970, *Physical Processes in Geology*, Freeman & Cooper, San Francisco, California, United States of America.

[15] Kafle, J., Pokhrel, P. R., Khattri, K. B., Kattel, P., Tuladhar, B. M., and Pudasaini, S. P., 2016, Landslide-generated tsunami and particle transport in mountain lakes and reservoirs, *Ann. Glaciol*, 57, 232-244.

[16] Kattel, P., Khattri, K. B., Pokhrel, P. R., Kafle, J., Tuladhar, B. M., and Pudasaini, S. P., 2016, Simulating glacial lake outburst floods with a two-phase mass flow model, *Ann. Glaciol.*, 57, 349-358.

[17] Kattel, P., and Tuladhar, B. M., 2018, Interaction of two-phase debris flow with lateral converging shear walls, *Journal of Nepal Mathematical Society*, 1(2), 40-52.

[18] Kowalski, J., 2008, *Two-phase Modeling of Debris Flows*, PhD Dissertation, University of Augsburg, Augsburg.

[19] Leipnik, R. B., 1992, Partial differential equations for eigenvalues: Sensitivity and perturbation analysis, *Austral. Math. Soc. Seri. B*, 34(4), 439-470.

[20] Liu, K. M., and Ortiz, E. L., 1986, Numerical solution of eigenvalue problems of partial differential equations with tau-lines method, *Comp. & Maths. with Appls.*, 12 B, 1153-1161.

[21] McCoy, S. W., Kean, J. W., Coe, J. A., Tucker, G. E., Staley, D. M., and Wasklewicz, T. A., 2012, Sediment entrainment by debris flows: In situ measurements from the headwaters of a steep catchment, *J. Geophys. Res.* 117(F03016).

[22] Mergili, M., Fischer, J.- T., Krenn, J., and Pudasaini, S. P., 2017, r.avaflow v1, an advanced open-source computational framework for the propagation and interaction of two-phase mass flow, *Geosci. Model Dev.*, 10, 553-569.

[23] Mergili, M., Schratz, K., Ostermann, A., and Fellin, W., 2012, Physically-based modeling of granular flows with Open Source GIS, *Nat. Hazards Earth Syst. Sci.*, 12, 187-200.

[24] Miller, D. J., 1960, Alaska Earthquake on July 10, 1958: Giant wave in Lituya Bay, *Bull. Seismol. Soc. Am.*, 50(2), 253-266.

[25] Miller, D. J., 1964, Alaska Earthquake on July 10, 1958: Giant wave in Lituya Bay, *Bull. Seismol. Soc. Am.*, 50(2), 253-266.

[26] Nessyahu, H., and Tadmor, E., 1990, Non-oscillatory central differencing for hyperbolic conservation laws, *J. Comput. Phys.*, 87, 408-463.

[27] Pitman, E. B., and Le, L., 2005, A two-fluid model for avalanche and debris flows, *Philos. Trans. R. Soc. A.*, 363, 1573-1602.

[28] Pokhrel, P. R., and Tuladhar, B. M., 2019, Determination of phase-eigenvalues by rational factorization and enhanced simulation of two-phase mass flow, *Journal of Nepal Mathematical Society*, 2(2), 61 - 77.

[29] Pokhrel, P. R., Khattri, K. B., Tuladhar, B. M., and Pudasaini, S. P., 2018, A generalized quasi two-phase bulk mixture model for mass flow, *Int. J. of Non-Linear Mech.*, 99, 229-239.

[30] Pokhrel, P. R., 2019, *Generalized Quasi Two-Phase Bulk Mixture Models for Mass Flow*, PhD Dissertation, School of Science, Kathmandu University, Nepal.

[31] Pokhrel, P. R., and Pudasaini, S. P., 2020, A simple stream function vorticity-formulation of mixture mass flow, *Int. J. of Non-Linear Mech.*, 121, 103317.

[32] Prager, W., and Drucker, D. C., 1952, Soil mechanics and plastic analysis or limit design, *Q. Appl. Math.*, 10(2), 157-165.

[33] Pudasaini, S. P., 2012, A general two-phase debris flow model, *J. of Geophysics Res.*, 117, F03010.

[34] Pudasaini, S. P., and Hutter, K., 2007, *Avalanche Dynamics: Dynamics of Rapid Flows of Dense Granular Avalanches*, Springer-Verlag, Berlin.

[35] Pudasaini, S. P., and Miller, S. A., 2012a, buoyancy induced mobility in two-phase debris flow, *American Institute of Physics Proceedings*, 1479, 149-152.

[36] Pudasaini, S. P., Wang, Y., and Hutter, K., 2005, Modeling debris flows down general channels, *Nat. Hazards Earth Syst. Sci.*, 5, 799-819.

[37] Regmi, N. R., Giardino, J. R., McDonald, E. V., and Vitek, J. D., 2015, A review of mass movement processes and risk in the critical zone of earth, *Developments in Earth Surface Processes*, 19, 319-362.

[38] Wang, W., and Shen, J., 2011, Eigenvalue problems of second order impulsive differential equations, *Computers and Mathematics with Applications*, 62(1), 142-150.

[39] Wang, Y., Pudasaini, S. P., Hsiau, S. S., and Hutter, K., 2005, Velocity measurements in dry granular avalanches using particle image velocimetry technique and comparison with theoretical predictions, *Physics of Fluid*, 27(1-2), 301-313.